Taylor, B., Huchon, P., Klaus, A., et al., 1999
Proceedings of the Ocean Drilling Program, Initial Reports Volume 180

2. *Data Report:* Marine Geophysical Surveys of the Woodlark Basin Region[1]

Andrew M. Goodliffe,[2] Brian Taylor,[2] and Fernando Martinez[2]

ABSTRACT

This report presents images of the marine geophysical (bathymetry, acoustic imagery, magnetics, gravity, and reflection seismic), land topographic, and earthquake data sets used to define and locate the sites drilled on Ocean Drilling Program Leg 180. We describe the processing of the data as well as the data products.

INTRODUCTION

The Woodlark Basin is a young marginal basin in the western Pacific that is both propagating westward into the Papuan Peninsula of New Guinea and being subducted eastward beneath the Solomon Islands (Fig. F1; Weissel et al., 1982). Extension is confined to a narrow region by the rheologically stronger oceanic lithosphere of the Solomon Sea to the north and the Coral Sea to the south. The pole of opening is nearby; therefore, major variations in the kinematic parameters and structural development (both continental and oceanic) are found within a small area. The spatial progression from continental rifting to seafloor spreading is kinematically equivalent to, and allows a study of, the temporal evolution of the rift-spreading system. These qualities make the Woodlark Basin an excellent place to study continental rifting, the initiation of seafloor spreading, and the evolution of a young ocean basin.

The purpose of this report is to document and display the marine geophysical and seismological data that were used to define the processes to be investigated and the location of the sites to be drilled dur-

F1. Topographic image of Woodlark Basin region, p. 10.

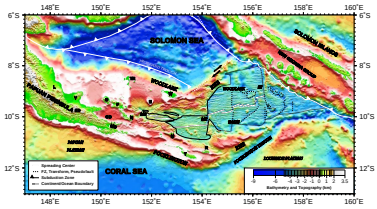

[1]Examples of how to reference the whole or part of this volume.

[2]School of Ocean and Earth Science and Technology, University of Hawaii, Honolulu, HI 96822, U.S.A.
andrew@soest.hawaii.edu

Ms 180IR-102

ing Ocean Drilling Program (ODP) Leg 180. We first discuss the data and processing methods, then illustrate the regional topographic, seismicity, magnetic, and gravity data products, and finally, present the multichannel seismic (MCS) reflection data proximal to the drilled sites.

GEOPHYSICAL DATA AND PROCESSING

We have compiled an extensive digital geophysical database for the Woodlark Basin region (Fig. F2; Table T1). We have full coverage swath bathymetry and acoustic imagery in the western Woodlark Basin and over much of the eastern Woodlark Basin. More widely spaced ship track data extend onto the margins of the eastern Woodlark Basin and into the Coral and Solomon Seas. Along-track gravity, magnetic, and MCS data are available for many cruises. Land topography and gravity data, as well as teleseismic earthquake locations and focal mechanisms, are also included.

F2. Geophysical database for Woodlark Basin region, p. 11.

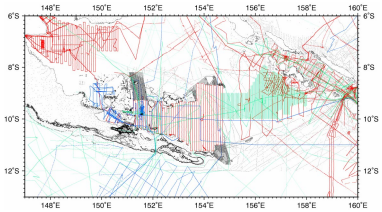

T1. Data sources for geophysical compilations, p. 19.

Historic bathymetric surveys are compiled as soundings on Royal Australian Navy and U.S. Defense Mapping Agency charts, many of which we have digitized. Critical hydrographic charts include 19th century British Admiralty surveys around the shoals and reefs bordering the basin, and the 1967–1968 *HMAS Moresby* survey that charted the region, including Moresby Transform and Moresby Seamount. A seismic sparker and bathymetry survey of Milne Bay was chartered in 1968 (Jongsma, 1972).

Satellite-navigated cruises in the region began with the 1970 Australian Bureau of Mineral Resources, Geology and Geophysics continental margin survey contracted to Compagnie Générale de Géophysique (Willcox, 1973). A reconnaissance survey of ridge subduction in the eastern Woodlark Basin–Solomon Islands region was completed in 1982 on the *Kana Keoki* (Taylor and Exon, 1987). This was followed in 1985 by a SeaMARC II sidescan and geophysical survey of the triple junction region on the *Moana Wave* (Crook et al., 1991; Crook and Taylor, 1994).

In 1992, on the *Maurice Ewing,* scientists completed a MCS, gravity, and Hydrosweep swath bathymetry survey around the D'Entrecasteaux Islands and in the western Woodlark Basin (Mutter et al., 1996). HAWAII-MR1 sidescan and geophysical surveys of the western Solomon Sea and Woodlark Basin were conducted on the *Moana Wave* in 1992 and April–May 1993, respectively (Galewsky and Silver, 1997; Taylor et al., 1995). These cruises included swath bathymetry and acoustic imagery, gravity, magnetic, and six-channel seismic data along north-south tracks, with a 5-nmi spacing. In August–September 1993, the Mineral Mining Agency of Japan conducted a seafloor mineral survey of the eastern Woodlark Basin using the *Hakurei Maru No. 2* (Deep Ocean Resource Development Co., 1995). Hydrosweep swath bathymetry and acoustic imagery and magnetic data were collected along north-south tracks with a spacing of 2.5 nmi. The combined surveys resulted in total bathymetry and acoustic imagery coverage of the entire spreading system, extending from margin to margin west of 154°45'E and farther east at least 50 km on either side of the spreading system.

In November 1995, as part of an ODP site survey, we completed a MCS survey of the region around Moresby Seamount on the *Maurice Ewing* (Taylor et al., 1996). Hydrosweep swath bathymetry and acoustic imagery and magnetic, and gravity data collected along track provided improved definition of Moresby Seamount. In addition, a transit track

crossed the eastern Woodlark Basin. Additional data from the U.S. National Geophysical Data Center (NGDC) archives and satellite gravity and predicted bathymetry values (Sandwell and Smith, 1995; Smith and Sandwell, 1997) complete our suite of marine geophysical data. MCS data were processed using Promax software. Compilation, processing, and display of data utilized the "GMT" software of Wessel and Smith (1995).

A complete bathymetric map of the Woodlark Basin region was compiled using swath bathymetry, wide-beam profiler data, and digitized depth soundings. Where data remained sparse, satellite-predicted bathymetry values were added (Smith and Sandwell, 1997). The data were initially median filtered and placed on a grid of 0.01° latitude and longitude. The higher resolution data, on a grid of 0.002°, was integrated with this data set. The final stage in the data compilation involved the addition of U.S. Geological Survey (USGS) 30″-arc grid topographic data of the islands and the Papuan Peninsula.

Processing of the HAWAII-MR1 acoustic imagery was conducted by the Hawaii Mapping Research Group (HMRG). In addition, we removed erroneous values at the nadir, used an asymmetric (0.1° across the ship track by 0.001° along the ship track) Gaussian filter to extrapolate data into the resulting data gap, and provided corrections to the across-track amplitude variation to improve the continuity of the high backscatter region associated with the spreading center. The final product was a 0.001° grid. The HAWAII-MR1 data were merged with *Hakurei Maru No. 2* Hydrosweep acoustic amplitude data from the eastern Woodlark Basin, also on a grid of 0.001°.

Shipboard magnetics data are primarily from the 1993 *Moana Wave* and *Hakurei Maru No. 2* surveys. The data from these cruises had no significant discrepancies between them and were used as a reference. Crossover corrections to other shipboard data were made by sampling the grid of the *Moana Wave* and *Hakurei Maru No. 2* data at the location points of the respective cruises. The average difference between data from each cruise and the grid of the reference data was removed on a cruise-by-cruise basis. The crossover corrected data were then median filtered and placed on a grid of 0.01°. The magnetic anomaly grid was resampled to 0.002° and inverted with the bathymetry grid to derive a magnetization solution assuming a 1-km-thick source layer that conforms to the seafloor, following the technique of Macdonald et al. (1980).

Shipboard free-air gravity anomaly data were crossover adjusted in a similar way to the magnetic data, and discrepancies were removed on a cruise-by-cruise basis with respect to the *Maurice Ewing* 1995 crossing of the Woodlark Basin. This cruise was used as a reference because of the high quality of its gravity data (collected with a BGM-3 gravity meter; Bell and Watts, 1986) and navigation (using the Global Positioning System), and because it crosses the entire basin from west to east, intersecting the track of most other cruises. First, the data from each cruise that had an intersection with the *Maurice Ewing* 1995 track were adjusted. Remaining cruises were adjusted by removing the average discrepancy of each of these with respect to the corrected ensemble of the first group. In the case of the *Moana Wave* 1993 cruise, intermittent problems with the gravimeter created abrupt offsets in the gravity data. Therefore, for this cruise, the data were divided into four segments bounded by the offsets, and each segment was adjusted individually to remove the discrepancy with respect to previously adjusted cruise data.

In addition to shipboard gravity data, we have also merged satellite altimetry-derived gravity data from Sandwell and Smith (1995) to help interpolate the gravity field between tracks. The gridded satellite altimetry-derived gravity data were sampled at the location of the adjusted ship data, and the average difference was removed from the satellite data. Next, a combined data set was compiled by using the adjusted shipboard measurements and gradual tapering to the corrected satellite-derived values over a distance of ~5 nmi. This was done to preserve the higher resolution of the ship data (Neumann et al., 1993) while taking advantage of the uniform coverage of the satellite data to interpolate between widely spaced ship tracks, primarily in the eastern basin.

Using the gridded bathymetry, the gravity effect of the seafloor topography was forward calculated, assuming a density contrast between the water and basement of 1800 $kg \cdot m^{-3}$, following Parker's (1973) method (using five terms). Because this method requires the observation plane (sea level) to be above all the relief, the gridded surface was truncated at a water depth of 100 m before the calculation. The gravity effect of the topography was then subtracted from the free-air anomalies to produce Bouguer anomalies. This calculation overestimates the gravity contribution of the topography where there is significant sediment thickness with lower densities than the crustal value we have adopted (2800 $kg \cdot m^{-3}$), thereby creating excessively negative anomalies in these areas. The Bouguer gravity anomaly map is particularly useful to examine the differences between the oceanic domains of the Woodlark Basin that have little sediment cover.

DATA DESCRIPTION

Morphology and Seismicity

The Woodlark and Pocklington Rises, which are topped by reefs, shoals, and islands in the west, narrow and deepen eastward (Fig. **F1**). The rises separate the seafloor of the Woodlark Basin from that of the surrounding Solomon and Coral Seas, respectively. The rises merge westward with the Papuan Peninsula of New Guinea, where the central range is more than 3500 m above sea level (Figs. **F1, F3**). Other high topography is associated with the gneissic domes of the Suckling-Daymon massif (Davies, 1980) and of the D'Entrecasteaux Islands (Goodenough, Fergusson, Normanby; Davies and Warren, 1988) and, to a lesser extent, by volcanoes along the north coast of the Peninsula, such as Mounts Lamington and Victory that have erupted this century (Smith, 1981). The latter are part of a Quaternary calc-alkaline arc associated with southward subduction at the Trobriand Trough (Smith, 1981). The Trobriand Trough terminates at 153.5°E, northeast of which the bathymetry and seismicity define a right-lateral transform fault along the northern margin of the Woodlark Rise (Fig. **F3**).

Because of the generally thin sediment cover, the pattern of faulting and the transition from block-faulted continental lithosphere of the Woodlark and Pocklington Rises to the rugged, seismically diffracting, oceanic lithosphere of the Woodlark Basin are readily apparent in swath bathymetry and seismic reflection data (Hill et al., 1984; Goodliffe et al., 1993, 1997; Taylor et al., 1995, in press). The continent-ocean boundary defined by Goodliffe (1998) and Taylor et al., (in press) is depicted in Figures **F1, F3, F4, F5, F6,** and **F7.** The extent of oceanic lithosphere decreases westward and terminates at 151.7°E where it abuts Moresby

F3. Topography, bathymetry, and seismicity of Papuan Peninsula–Woodlark Basin region, **p. 12**.

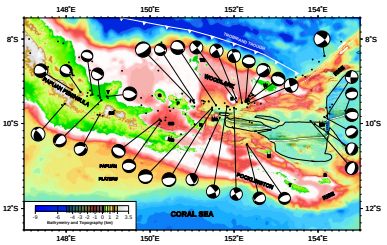

Seamount. Further west, Milne and Goodenough Bays are full and half graben respectively, produced by continental rifting (Milsom and Smith, 1975; Mutter et al., 1996). Earthquake seismicity and focal mechanisms (Fig. F3) attest to (1) crustal tensional seismicity as far west as 148°E (Weissel et al., 1982; Abers, 1991; Abers et al., 1997) and (2) rifting of the continental margins (to 153°E) continuing after the onset of seafloor spreading (Taylor et al., 1995). The seismicity is characterized by normal and strike-slip events, with northerly T-axes. Several of the normal fault focal mechanisms permit slip on shallow-dipping (25°–35°) planes (Abers, 1991; Abers et al., 1997).

The neo-volcanic zone of the axis of seafloor spreading is defined by strong acoustic backscatter (Fig. F3). The spreading center sharply crosscuts the majority of the oceanic seafloor fabric. Goodliffe et al. (1997) showed that the crosscutting relationship is due to an extremely rapid reorientation of the spreading direction ~80 ka. There are many nontransform offsets of the spreading axis, as well as major transform offsets, such as Moresby and Simbo Transforms (Figs. F1, F3). Contrasting the morphology west vs. east of Moresby Transform (Martinez et al., 1996), the seafloor is smoother (100–200 m vs. 200–400 m relief), the spreading center has a rifted axial high in contrast to axial valleys, and the ridge flanks are systematically shallower by ~500 m since the onset of spreading. The lack of a linear region of strong acoustic backscatter east of Simbo Transform (Goodliffe, 1998), together with the northward progression of seafloor ages (see below), confirms the suggestion of Taylor and Exon (1987) and Crook and Taylor (1994) that the spreading center has been subducted there.

Magnetization and Seafloor Age

The magnetic data show that the formerly contiguous, eastward extensions of the Papuan Peninsula (the Woodlark and Pocklington Rises) were separated as the Woodlark spreading center propagated westward during the last 6 Ma (Weissel et al., 1982; Taylor and Exon, 1987; Taylor et al., 1995). Our magnetization solution is presented in Figure F4, and the seafloor spreading magnetic lineations inferred from it by Goodliffe (1998) and Taylor et al. (in press) are shown in Figure F5. We adopt the magnetic time scale of Cande and Kent (1995). The oldest magnetic chron identified is 3A.1 (5.89–6.14 Ma), which occurs in the easternmost basin immediately south of Chron 3.4. Goodliffe (1998) reconstructed the seafloor spreading history and Taylor et al. (in press) derived the following poles of opening: 2.437°/m.y. about 144°E, 12°S between 0.0 and 0.52 Ma and 4.234°/m.y. about 147°E, 9.3°S before 0.52 Ma. The data confirm and quantify the observation by Weissel et al. (1982) that the magnetic anomaly amplitudes are greater in the western basin than in the eastern basin. We find that east of Moresby Transform root-mean-square magnetic field and seafloor magnetization variations (Fig. F4) are 136 nT and 4.2 $A \cdot m^{-1}$ respectively, whereas west of Moresby Transform they are 273 nT and 6.6 $A \cdot m^{-1}$.

Gravity Anomalies

The free-air gravity field of the Woodlark Basin area (Fig.F6) broadly reflects the bathymetry, with a few notable exceptions associated with sedimentary basins. Presently active (e.g., Trobriand Trough) and former (e.g., Pocklington Trough) trenches (Davies et al., 1984) are marked by prominent gravity lows. Where the young lithosphere of the

F4. Seafloor magnetization of Woodlark Basin, p. 13.

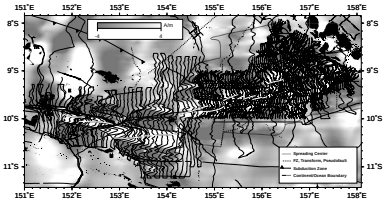

F5. Seafloor spreading magnetic lineations, p. 14.

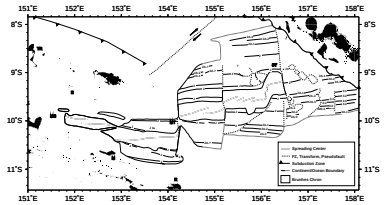

F6. Free-air gravity anomaly map, p. 15.

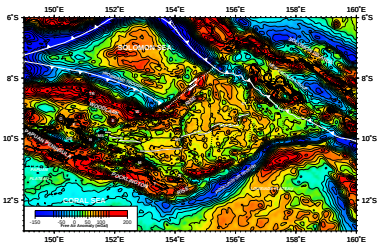

Woodlark Basin is being subducted beneath the New Georgia Group of the Solomon Islands, the islands are paralleled on the basin side by a 20–30 mGal relative high. Gravity lows with modest bathymetric expression are located in the New Georgia Basin area of the Solomon Islands and surrounding the D'Entrecasteaux Islands (Goodenough-Normanby). Of the latter lows, those to the south are associated with rifts such as Goodenough Basin. To the north, they reflect depocenters of the Miocene forearc basin. The depocenters are located south of the outer forearc basement high marked by the strong positive anomaly linking the Woodlark and Trobriand Islands. The eastern Woodlark Basin spreading centers are characterized by 10–20 mGal axial lows relative to flanking highs, whereas the western basin is characterized by a free-air gravity high along the spreading axis (except in the segment that approaches Moresby Seamount).

Bouguer gravity anomalies are shown in Figure F7. Removal of the topographic contribution to the gravity has significantly simplified the gravity anomalies, accounting for much of the short-wavelength variations seen in the free-air anomalies. Regionally, the oceanic lithosphere of the Solomon Sea and Woodlark and Coral Sea Basins is associated with Bouguer gravity highs, which is in contrast to the surrounding continental and arc lithosphere lows. Within the Woodlark Basin oceanic lithosphere there is a decreasing westward gradient in the Bouguer anomaly, as well as a 30-mGal step down westward across the Moresby Transform (Martinez et al., 1996). Relative lows paralleling the Woodlark-Trobriand residual high reflect the Trobriand Trough accretionary prism to the north and the Miocene forearc basin to the south.

F7. Bouguer anomaly map of Woodlark Basin region, p. 16.

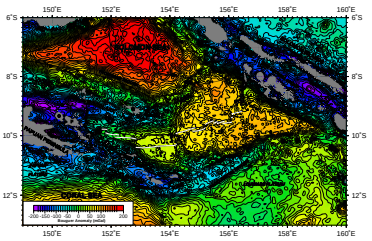

Seismic Reflection Data

Of the several MCS data sets available to us for the Woodlark Basin, we present in Figure F8 only those sections that were used to locate the sites drilled on ODP Leg 180. Some of these data have been described in Taylor et al. (1996, in press), and additional sections are presented in Mutter et al. (1996) and Abers et al. (1997). The MCS data image the structure and stratigraphy of

1. Moresby Seamount, capped by a normal-faulted sedimentary sequence that is over 1.5 s (two-way traveltime) thick, and bounded to the north by a low-angle (~30°) normal fault that is best imaged on the eastern lines (Taylor et al., 1996);
2. The Woodlark rift basin to the north of Moresby Seamount, with its sedimentary fill over 2 km thick, bounded on the north by an antithetic fault dipping ~45°S; and
3. The downflexed northern margin with a thinner synrift sequence unconformably above north-dipping reflectors, inferred by Taylor et al. (1996) to be a Miocene forearc basin and basement sequence.

F8. Site survey multichannel seismic data, p. 17.

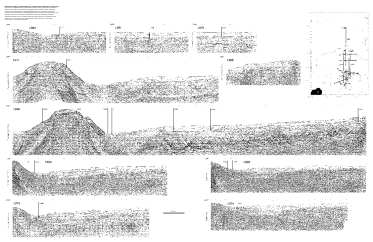

F9. Isopach map of synrift sediments, p. 18.

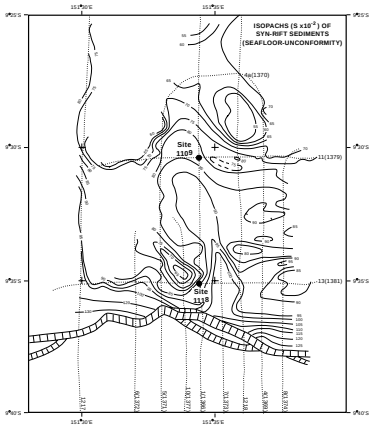

These data are interpreted in terms of drilling objectives and site locations in "Drilling Area," p. 7, in the "Background and Regional Setting" chapter. Before Leg 180, we constructed an isopach map of the synrift sedimentary section in the vicinity of Sites 1109 and 1118 (Fig. F9) from the grid of all available MCS data. When account is taken of the regional subsidence and southward tilting of the angular unconformity, the data reveal a paleoerosional surface with a north-northwest–trending chan-

nel in the vicinity of Site 1109 and flanking isolated highs, such as those drilled at Site 1118.

ACKNOWLEDGMENTS

This work was supported by the US NSF-ODP and JOI-USSSP. Primary data were collected on cruises of the *Moana Wave, Hakurei Maru No. 2,* and *Maurice Ewing*. We thank the Metal Mining Agency of Japan and the South Pacific Applied Geoscience Commission for providing Hydrosweep and magnetics data from the eastern Woodlark Basin. Reviews by Philippe Huchon and Garry Karner helped improve the manuscript. SOEST contribution # 4710.

REFERENCES

Abers, G.A., 1991. Possible seismogenic shallow-dipping normal faults in the Woodlark-D'Entrecasteaux extensional province, Papua New Guinea. *Geology,* 19:1205–1208.

Abers, G.A., Mutter, C.Z., and Fang, J., 1997. Shallow dips of normal faults during rapid extension: earthquakes in the Woodlark-D'Entrecasteaux rift system, Papua New Guinea. *J. Geophys. Res.,* 102:15301–15317.

Bell, R.E., and Watts, A.B., 1986. Evaluation of the BGM-3 sea gravity meter system on board R/V *Conrad. Geophysics,* 51:1480–1493.

Cande, S.C., and Kent, D.V., 1995. Revised calibration of the geomagnetic polarity timescale for the Late Cretaceous and Cenozoic. *J. Geophys. Res.,* 100:6093–6095.

Crook, K.A.W., and Taylor, B., 1994. Structure and Quaternary tectonic history of the Woodlark triple junction, Solomon Islands. *Mar. Geophys. Res.,* 16:65–89.

Crook, K.A.W., Taylor, B., and Falvey, D.A., 1991. Woodlark Triple Junction, Solomon Islands, SeaMARC II sidescan sonar imagery and bathymetry, 1:250,000. In *Pacific Seafloor Atlas:* Honolulu (Hawaii Inst. Geophys.), 9.

Davies, H.L., 1980. Folded thrust fault and associated metamorphics in the Suckling-Dayman massif, Papua New Guinea. *Am. J. Sci.,* 280-A:171–191.

Davies, H.L., Symonds, P.A., and Ripper, I.D., 1984. Structure and evolution of the southern Solomon Sea region. *BMR J. Aust. Geol. Geophys.,* 9:49–68.

Davies, H.L., and Warren, R.G., 1988. Origin of eclogite-bearing, domed, layered metamorphic complexes ("core complexes") in the D'Entrecasteaux islands, Papua New Guinea. *Tectonics,* 7:1–21.

Deep Ocean Resource Development Co., 1995. Woodlark Basin. In *South Pacific Seafloor Atlas:* Tokyo (S. Pacif. Appl. Geosci. Comm.), 10–11.

Galewsky, J., and Silver, E.A., 1997. Tectonic controls on facies transitions in an oblique collision: the western Solomon Sea, Papua New Guinea. *Geol. Soc. Am. Bull.,* 109:1266–1278.

Goodliffe, A.M., 1998. The rifting of continental and oceanic lithosphere: observations from the Woodlark Basin [Ph.D. thesis]. Univ. Hawaii, Honolulu.

Goodliffe, A.M., Taylor, B., Hey, R.N., and Martinez, F., 1993. Seismic images of continental breakup in the Woodlark Basin, Papua New Guinea. *Eos,* 74:606.

Goodliffe, A.M., Taylor, B., Martinez, F., Hey, R.N., Maeda, K., and Ohno, K., 1997. Synchronous reorientation of the Woodlark Basin spreading center. *Earth Planet. Sci. Lett.,* 146:233–242.

Hill, P.J., Reid, R., and Buleka, J. 1984. Marine geophysical survey of the west Woodlark Basin, M.V. Tapini, 1984—cruise report. *Bur. Miner. Resour. Aust. Rec.,* 32.

Jongsma, D., 1972. Marine geology of Milne Bay, eastern Papua. *Bull.—Bur. Miner. Resour., Geol. Geophys. (Aust.),* 125:35–54.

Macdonald, K.C., Miller, S.P., Huestis, S.P., and Spiess, F.N., 1980. Three-dimensional modeling of a magnetic reversal boundary from inversion of deep-tow measurements. *J. Geophys. Res.,* 85:3670–3680.

Martinez, F., Taylor, B., and Goodliffe, A.M., 1996. Variations in bathymetry and gravity between the eastern and western Woodlark basin: indications of a rift-induced thermal anomaly? *Trans. Am. Geophys. Union,* 77(Suppl.):706.

Milsom, J., and Smith, I.E., 1975. Southeastern Papua: generation of thick crust in a tensional environment? *Geology,* 3:117–120.

Mutter, J.C., Mutter, C.Z., and Fang, J., 1996. Analogies to oceanic behavior in the continental breakup of the western Woodlark Basin. *Nature,* 380:333–336.

Neumann, G.A., Forsyth, D.W., and Sandwell, D., 1993. Comparison of marine gravity from shipboard and high-density satellite altimetry along the Mid-Atlantic Ridge, 30.5°–35.5°S. *Geophys. Res. Lett.,* 20:1639–1642.

Parker, R.L., 1973. The rapid calculation of potential anomalies. *Geophys. J. R. Astron. Soc.,* 31:447–455.

Sandwell, D.T., and Smith, W.H.F., 1995. Marine gravity from satellite altimetry [Online]. Available by anonymous ftp: <ftp://topex.ucsd.edu/pub/global_grav_2min/world_grav.img.7.2> [Cited 1998-11-09].

Smith, I.E.M., 1981. Young volcanoes in eastern Papua New Guinea. *Mem.—Geol. Surv. Papua N. G.,* 10:257–265.

Smith, W.H.F., and Sandwell, D.T., 1997. Global seafloor topography from satellite altimetry and ship depth soundings. *Science,* 277:1956–1962.

Taylor, B., and Exon, N.F., 1987. An investigation of ridge subduction in the Woodlark-Solomons region: introduction and overview. *In* Taylor, B., and Exon, N.F., *Marine geology, geophysics, and geochemistry of the Woodlark Basin—Solomon Islands*. Circum-Pac. Counc. Energy Miner. Resour., Earth Sci. Ser., 7:1–24.

Taylor, B., Goodliffe, A.M., and Martinez, F., in press. How continents break up: insights from Papua New Guinea. *J. Geophys. Res.,* 104.

Taylor, B., Goodliffe, A.M., Martinez, F., and Hey, R.N., 1995. Continental rifting and initial seafloor spreading in the Woodlark Basin. *Nature,* 374:534–537.

Taylor, B., Mutter, C., Goodliffe, A., and Fang, J., 1996. Active continental extension: the Woodlark Basin. *JOI/USSAC Newsl.,* 9:1–4.

Weissel, J.K., Taylor, B., and Karner, G.D., 1982. The opening of the Woodlark basin, subduction of the Woodlark spreading system, and the evolution of northern Melanesia since mid-Pliocene time. *Tectonophysics,* 87:253–277.

Wessel, P., and Smith, W.H.F., 1995. New version of the generic mapping tools released. *Eos,* 76:329.

Willcox, J.B., 1973. Preview report for the marine geophysical survey of the Gulf of Papua and the Bismarck Sea. *Bur. Miner. Resour. Aust. Rec.,* 38.

Figure F1. A shaded topographic image of the Woodlark Basin region showing the major physiographic features and active plate boundaries. The tectonic elements defined in the legend are from Goodliffe (1998) and Taylor et al., (in press) and are reproduced on Figures **F3,** p. 12, **F4,** p. 13, **F5,** p. 14, **F6,** p. 15, and **F7,** p. 16. E = Egum Atoll, G = Goodenough Island, GB = Goodenough Basin, F = Fergusson Island, L = Mount Lamington, M = Misima Island, MB = Milne Bay, MS = Moresby Seamount, MT = Moresby transform fault, N = Normanby Island, R = Rossel Island, SD = Suckling-Daymon massif, ST = Simbo transform fault, T = Tagula Island, TR = Trobriand Islands, V = Mount Victory, and W = Woodlark Island.

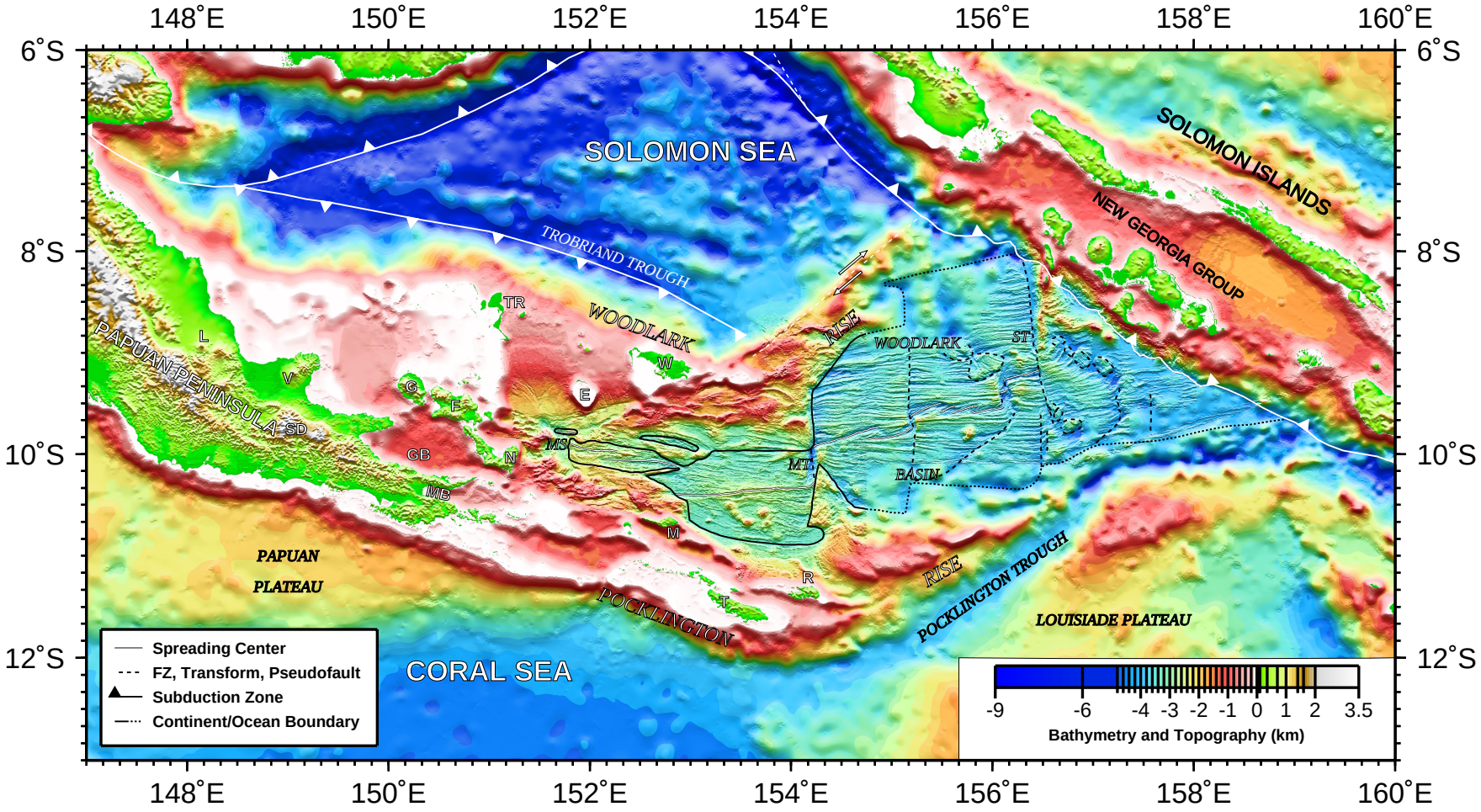

Figure F2. Lines and points locate our digital geophysical database for the Woodlark Basin region (see Table **T1,** p. 19, for data types). The data sources are color coded: red = SOEST, University of Hawaii; blue = LDEO, Columbia University; black = land gravity measurements and data digitized from charts, green = other institutions.

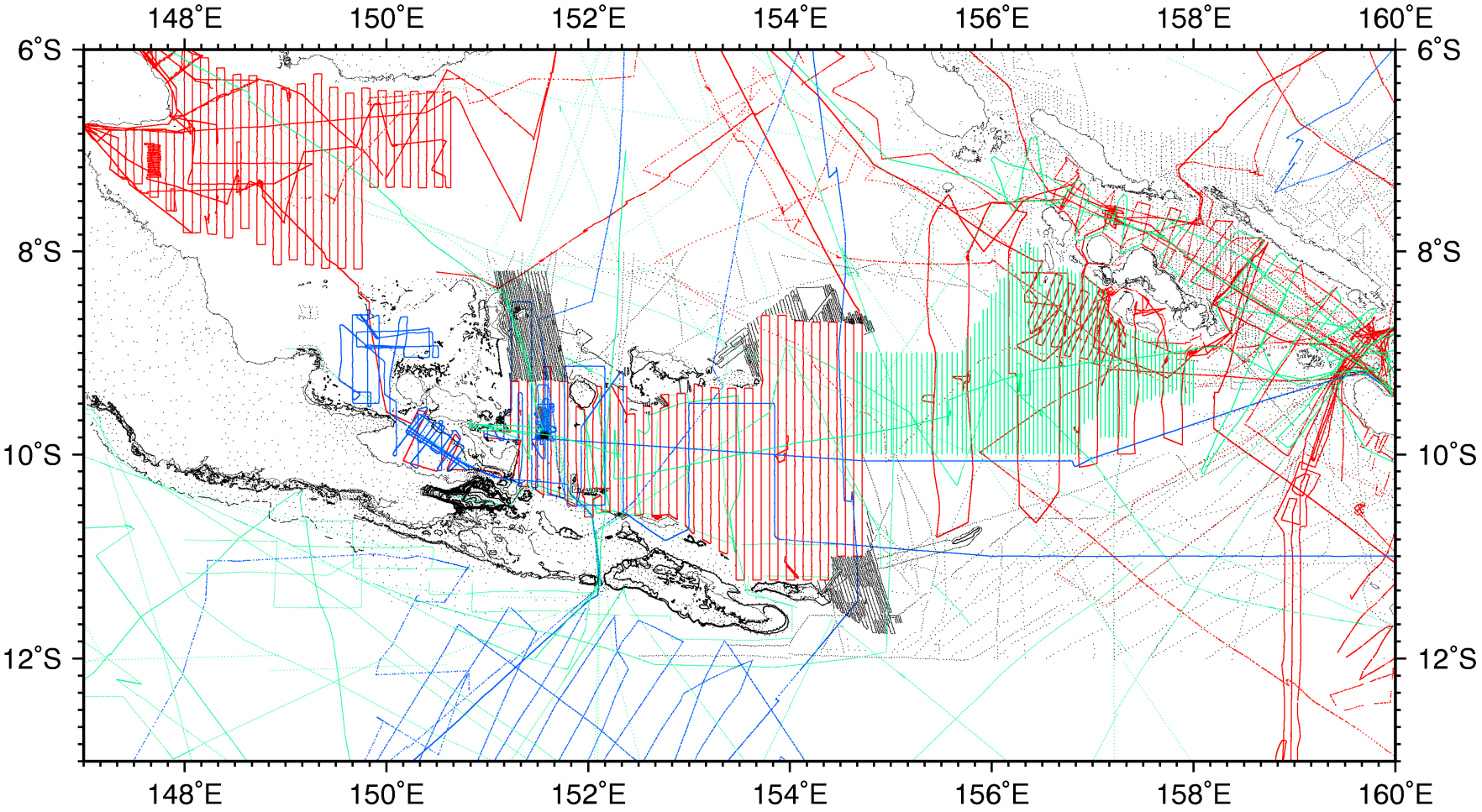

Figure F3. Topography and bathymetry of the Papuan Peninsula-Woodlark Basin region with acoustic imagery superimposed in the Basin. The neo-volcanic zone of the spreading center is indicated by the region of strong (dark) acoustic backscatter. Shallow earthquake seismicity (solid circles) and associated focal mechanisms (Abers, 1991; Abers et al., 1997) indicate tensional seismicity as far west as 148°E. See Figure F1, p. 10, for an explanation of tectonic symbols and place abbreviations.

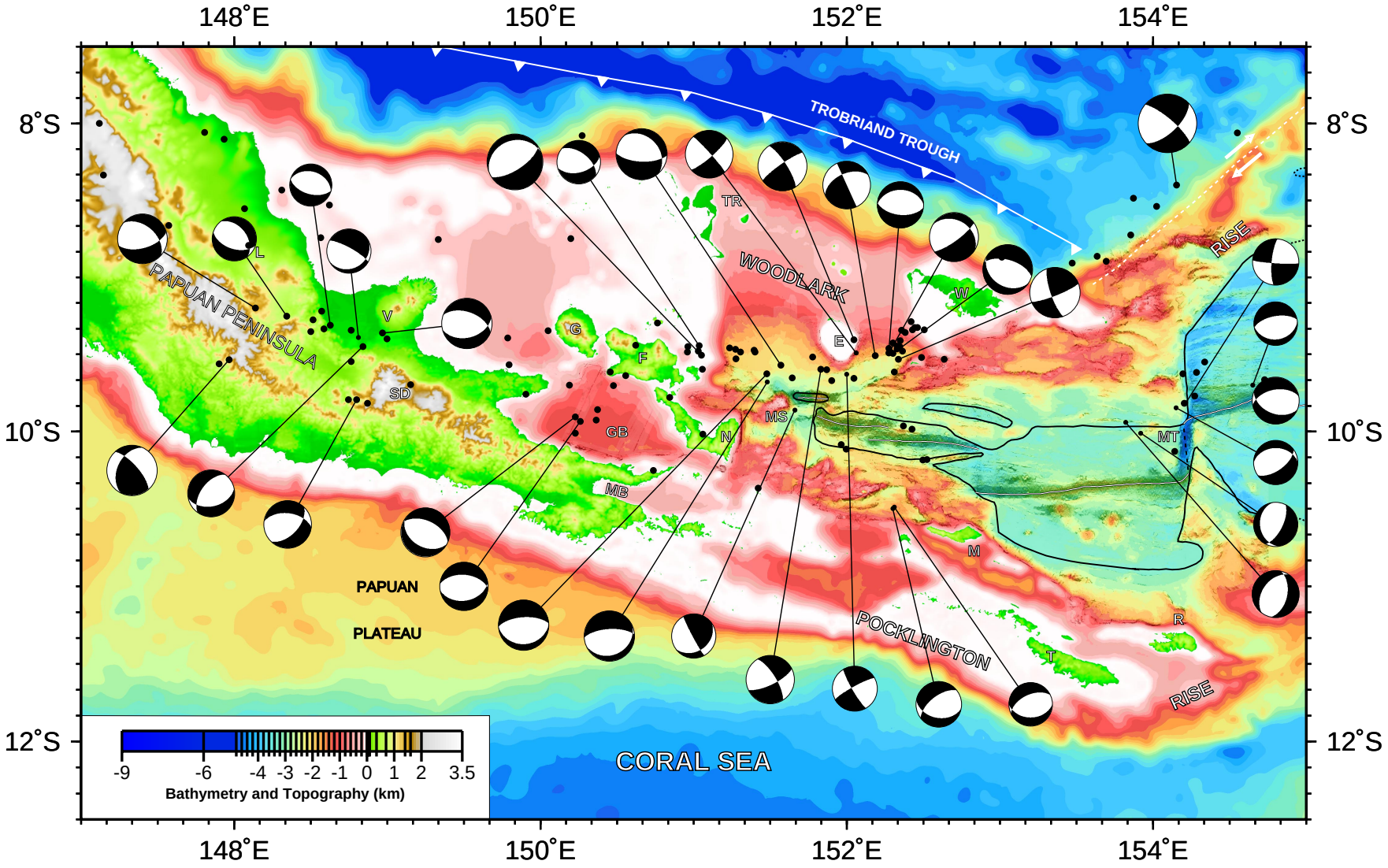

Figure F4. Seafloor magnetization of the Woodlark Basin. Magnetization profiles along track are plotted positive to the east. See Figure **F1,** p. 10, for place abbreviations.

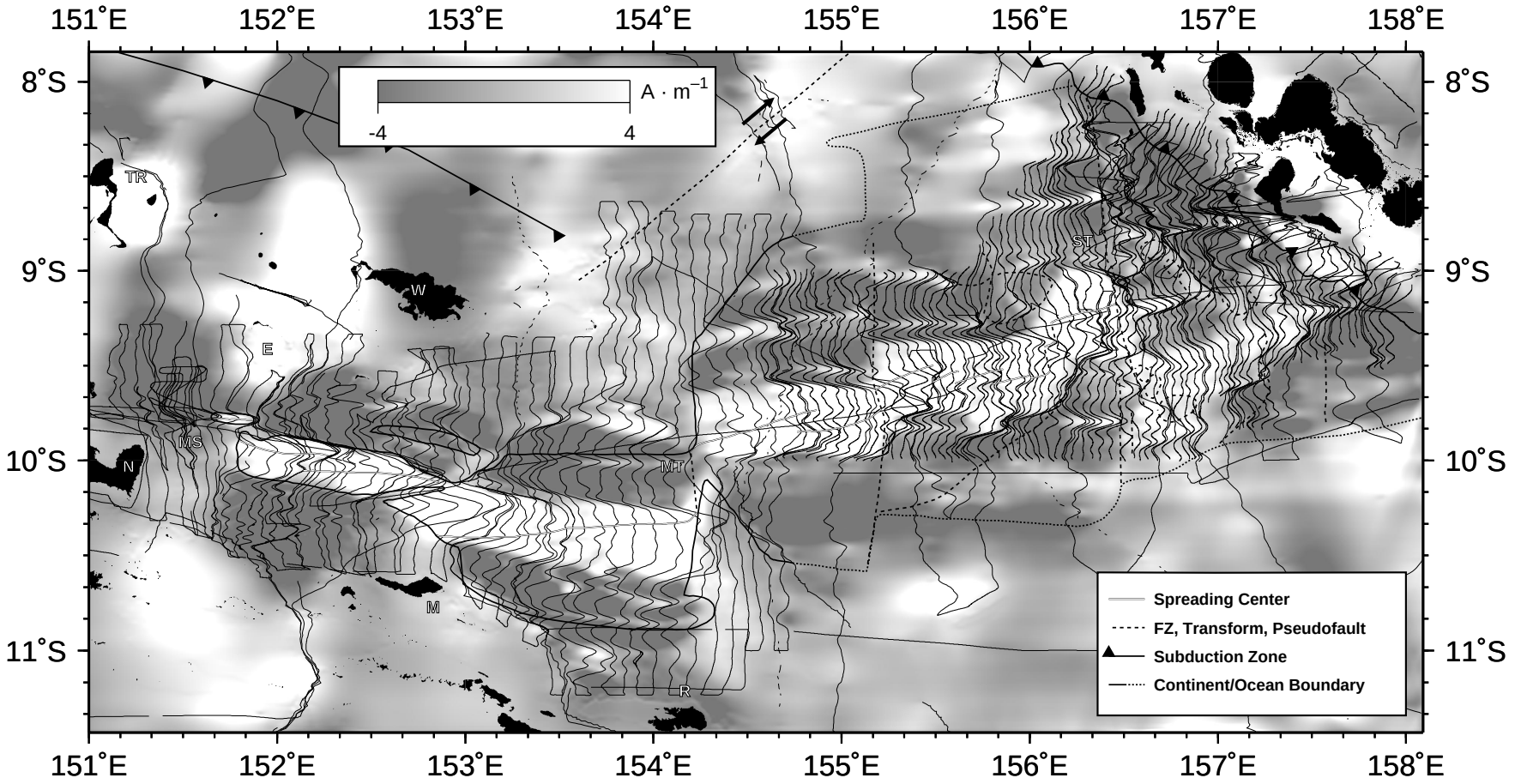

Figure F5. Seafloor spreading magnetic lineations as inferred by Goodliffe (1998) and Taylor et al., (in press). Normal polarity chrons are labeled following the convention of Cande and Kent (1995), except for Chron 1r.1 (Jaramillo), which is labeled as J. See Figure **F1,** p. 10, for place abbreviations.

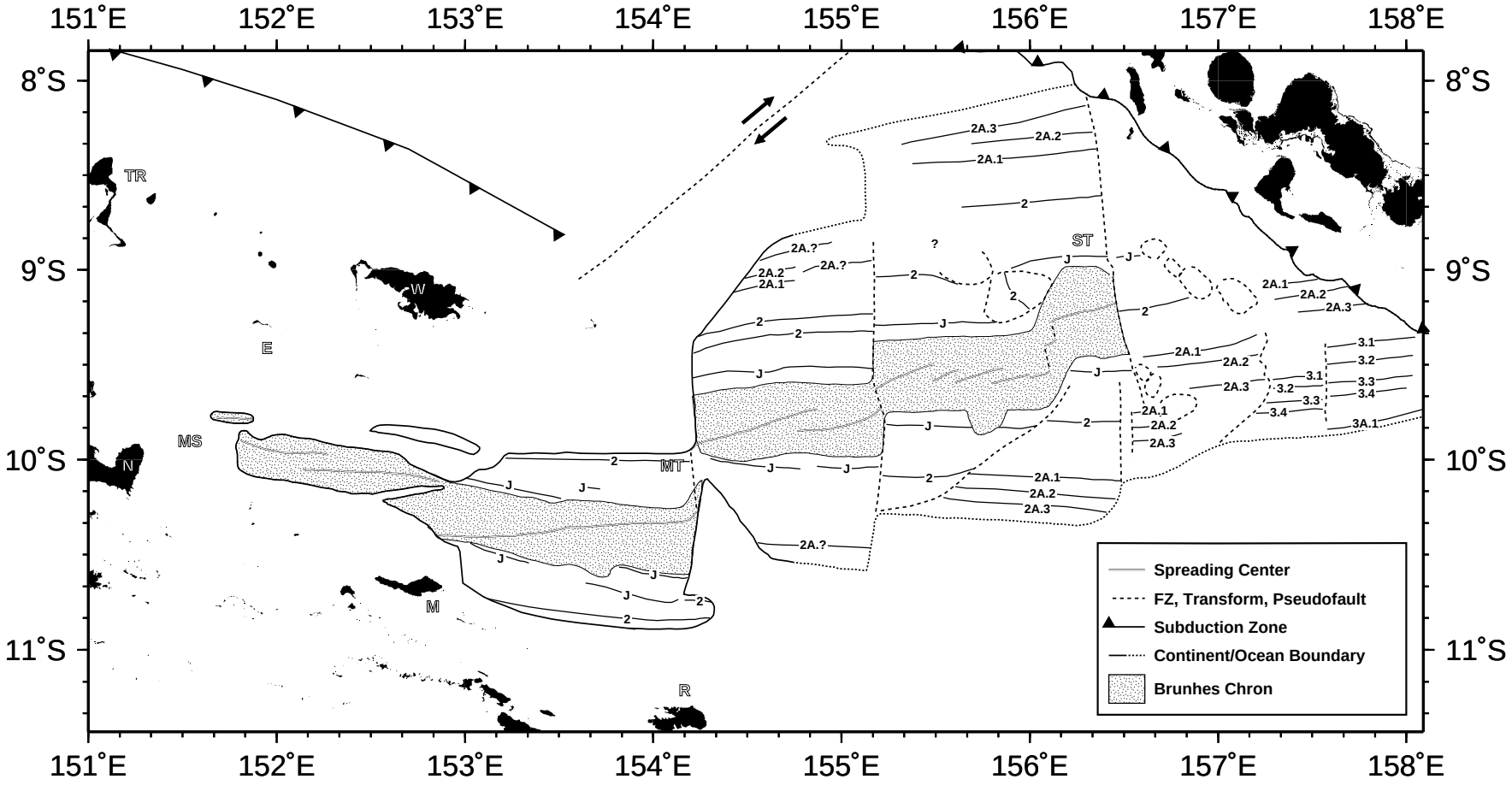

Figure F6. Free-air gravity anomaly map compiled from shipboard, land, and satellite altimetry-derived values. Contour interval is 20 mGal. See Figure F1, p. 10, for an explanation of tectonic symbols and place abbreviations.

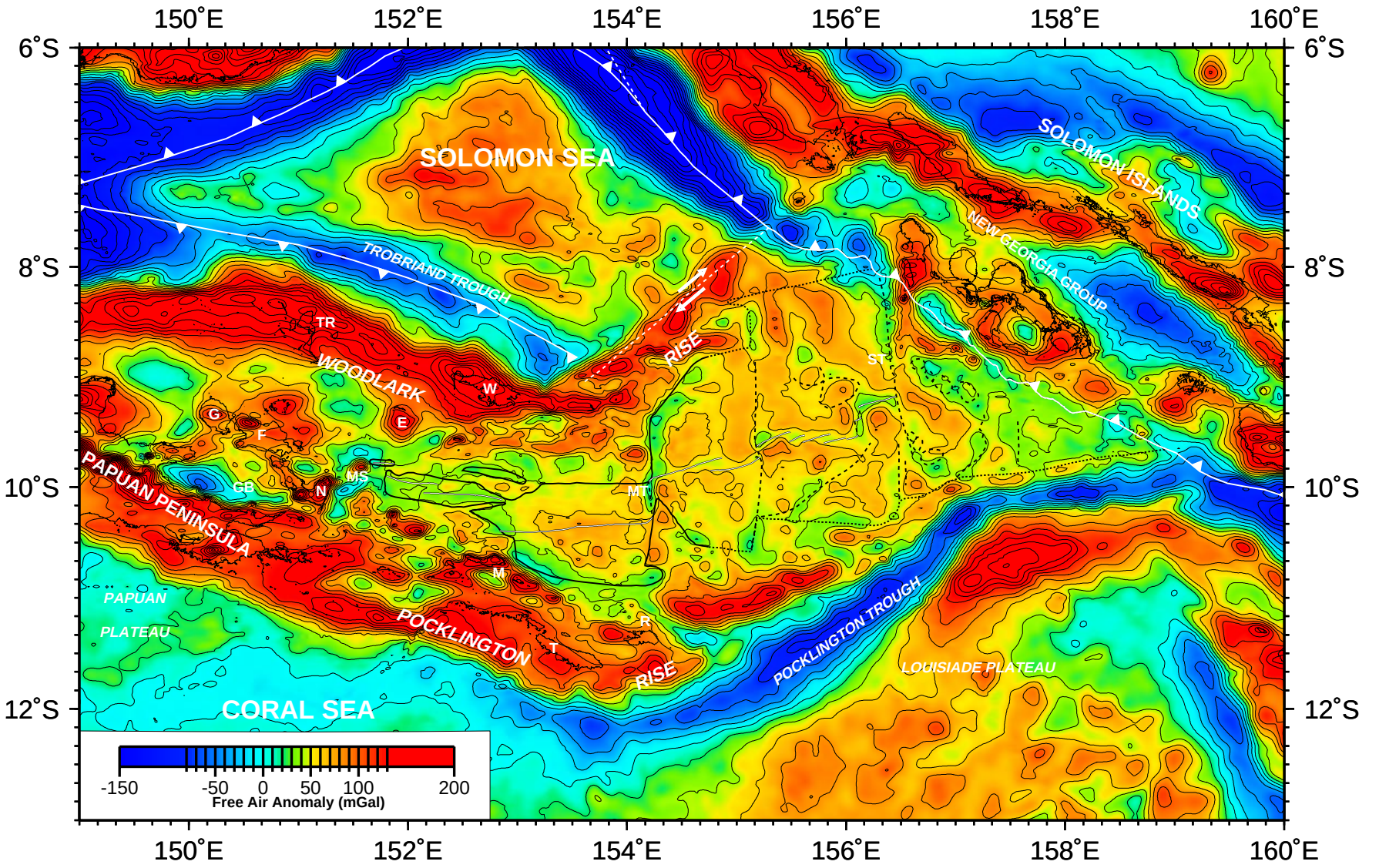

Figure F7. Bouguer anomaly map calculated using a density contrast of 1800 kg·m^{-3} between the water and basement. Contour interval is 10 mGal. See Figure **F1**, p. 10, for an explanation of tectonic symbols and place abbreviations.

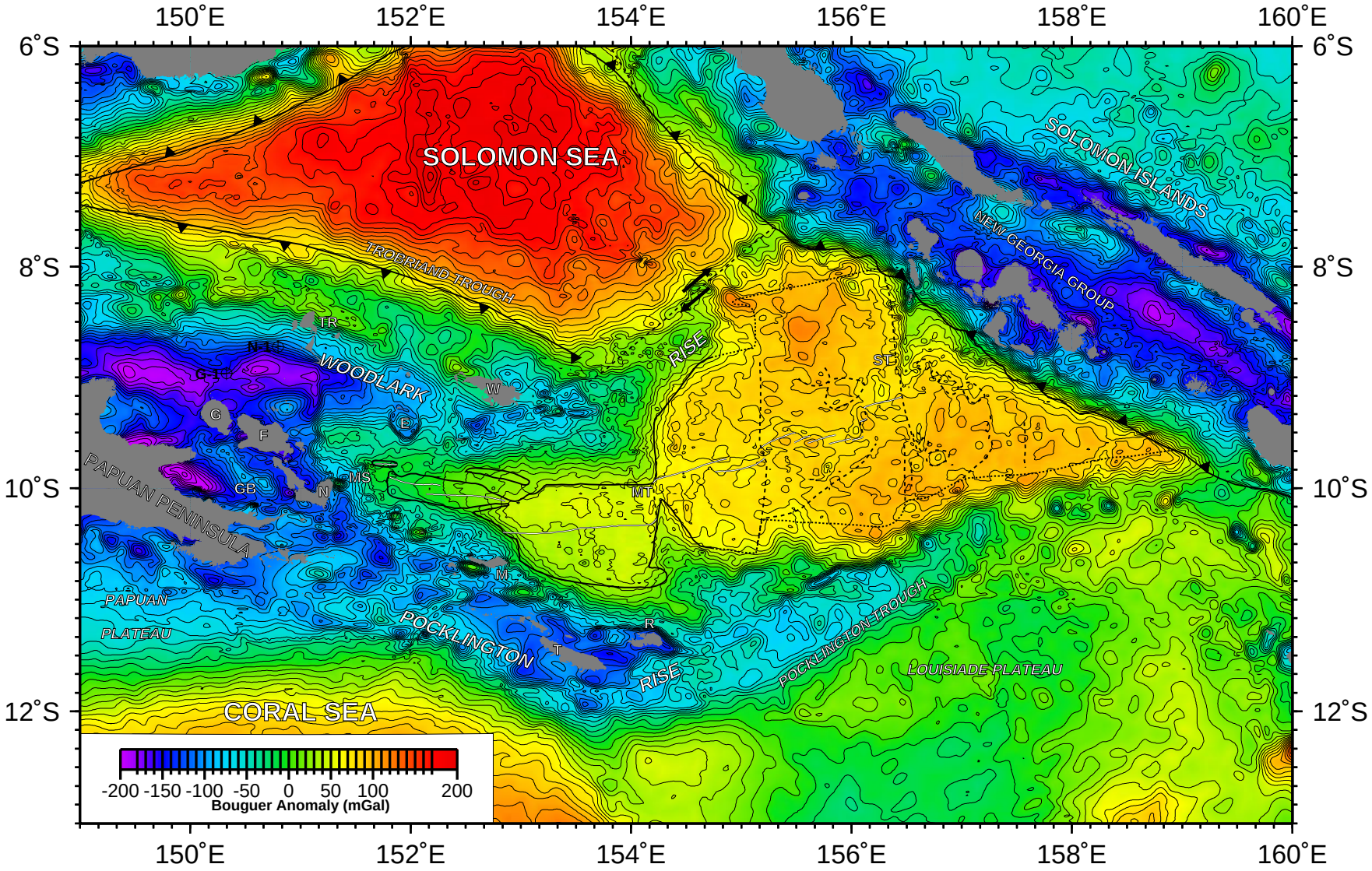

Figure F8. (An **oversized figure** accompanies this volume.) Site survey multichannel seismic (MCS) data showing the position of sites drilled. The data are presented as migrated time sections. Lines 1369 and 1374 are also presented as migrated depth sections. The inset shows the location of the MCS lines on a bathymetry base contoured every 200 m and labeled in km. Bold numbers label the sites and bold italic numbers label the MCS lines. Common depth points (CDP) are annotated every 1000 on the inset and every 100 above the MCS data.

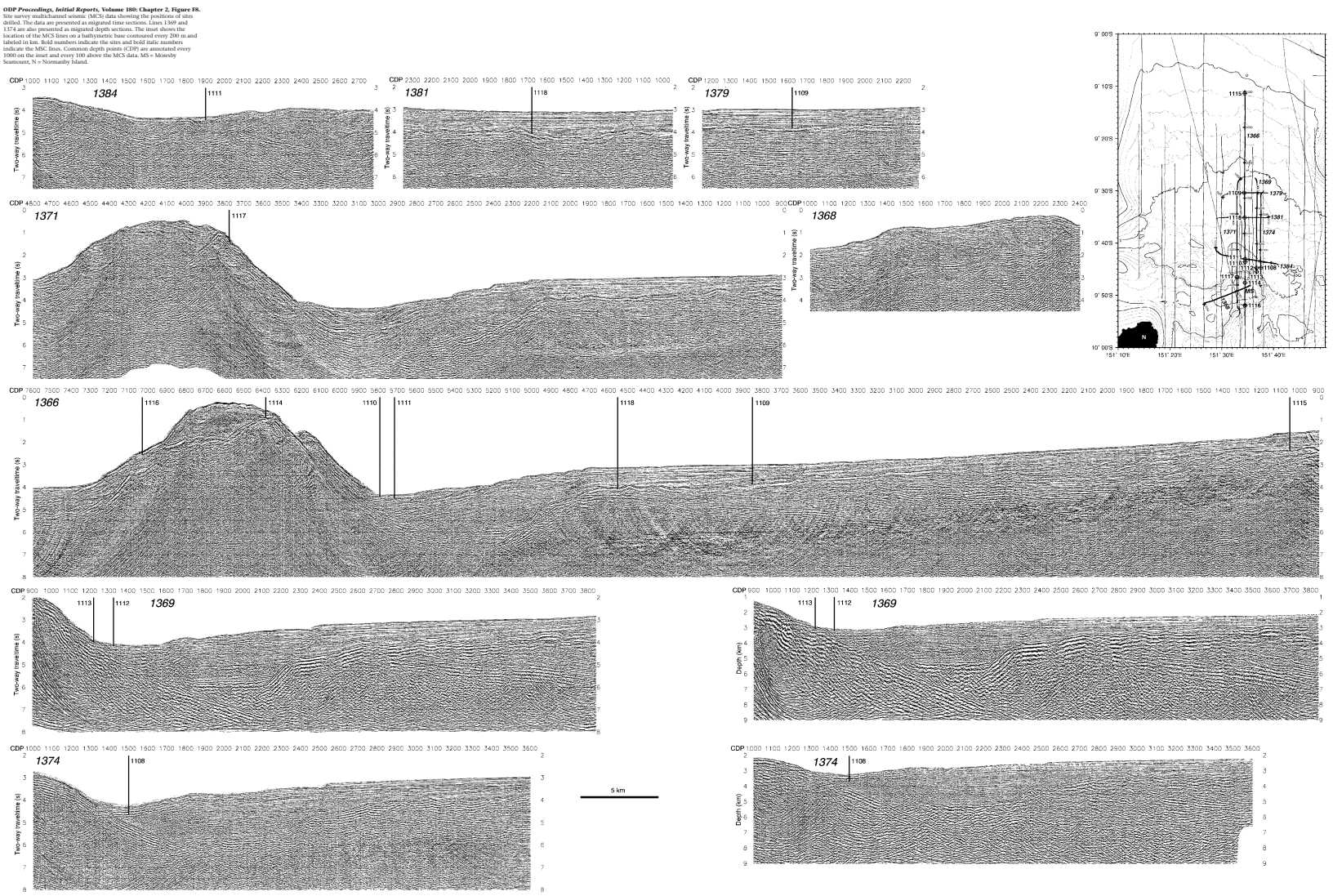

Figure F9. Isopach map of synrift sediments (i.e., between the seafloor and the angular unconformity above the forearc basin section) in the vicinity of Sites 1109 and 1118. Contours are labeled in hundredths of seconds of two-way traveltime. Dashed lines locate the MCS data used to construct the map. Hatched parallel lines mark the fault system that bounds the northern edge of the Woodlark rift basin.

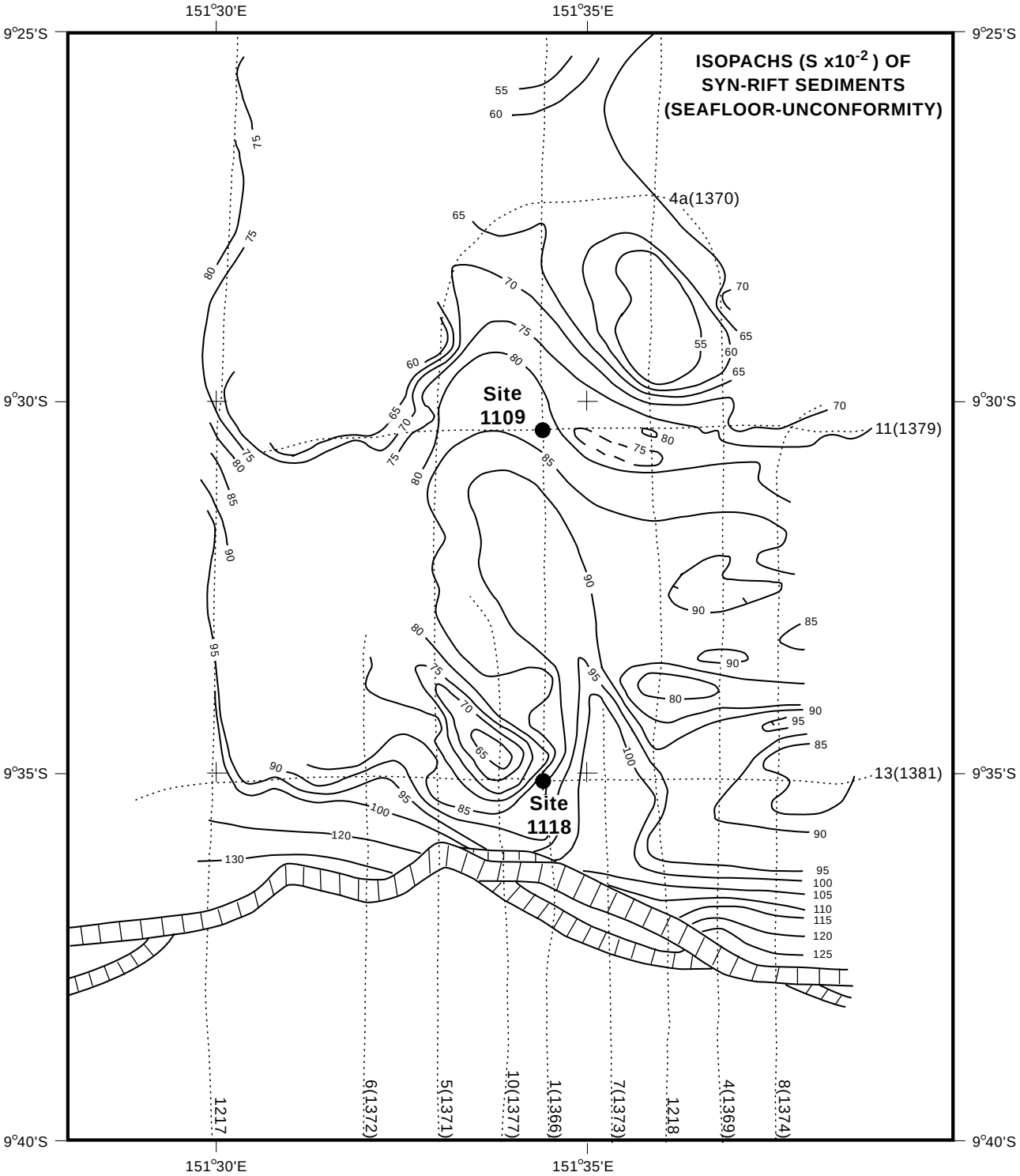

Table T1. Sources of cruise data used in our geophysical compilations. (Continued on next page.)

Cruise	Bathymetry	Magnetics	Gravity	Seismic reflection
SOEST, University of Hawaii				
MAH03			X	
MAHI7007	X			
MAHI7008	X			
MAHI7004	X	X	X	
KK7603	X			
MCH7901	X			
MCH7903	X			
MCH8101	X			
MCH8102	X			
MCH8103	X			
MCH8104	X			
KK8203	X	X	X	A
KK8205	X			
KK8206	X			
MW8517	SW	X	X	A
MW8601	X			
MW9004	X			
MW9005	X			
MW9108	X			
MW9204	SW	X	X	D
MW9303	X			
MW9304	SW	X	X	D
LDEO, Columbia University				
C1007	X	X	X	A
V2407		X	X	A
V2408	X	X	X	A
V2813	X			A
V3313	X	X	X	A
EW9203	SW	X	X	M
EW9510	SW	X	X	M
Woods Hole Oceanographic Institute				
CH100L08	X	X	X	
U.S. Geological Survey				
L782SP	X	X		
L941SP			X	
L944SP			X	
L984SP			X	
Scripps Institute of Oceanography				
NOVA04AR	X			
ERDC04WT	X			
PPTU06WT	X	X		
DSDP21GC	X			
DSDP30GC	X	X		
NOVA02HO	X			
LUSI05HO	X			
DSDP31	X			
Texas A&M University				
ODP133JR		X		
U.S. Government				
BB12B	X	X		A
PM061		X		
Australian Bureau of Mineral Resources				
TAPIN	X	X		A
BMR5A	X	X	X	D
BMR14	X		X	D
Russia				
DME18			X	
VI49	X		X	
France, Orstom				
AUS318	X	X		M
AUS4	X	X		
University of Tokyo				
KH6804-D	X			
KH7104	X	X	X	

Table T1 (continued).

Cruise	Bathymetry	Magnetics	Gravity	Seismic reflection
KH7304	X		X	
UM6402-A	X	X		
UM6402-C	X			
UM66-A	X	X		
UM67	X	X		
Mineral Mining Agency of Japan				
HM9308	SW	X		
United Kingdom				
DDAMP	X		X	

Note: SW = swath bathymetry, A = analog, D = digital, M = multichannel seismic.